Comparison of different methods for preventing the infill's detrimental effects in the infilled steel frames

Saher Elkhoreeby, Mohamed A. Saker, Tarek M. khalifa, Mohammed Eladly*

[#] *Department of Structural Engineering, Faculty of Engineering, Tanta University*
Tanta, Egypt

[*]Eladly@ymail.com

Abstract *The presence of infill panels in buildings with concrete or steel frames can lead to conflicting effects on the structural response, depending on the mechanical properties, the geometrical distribution of infills and the interaction with structural elements. Traditionally, the infill walls are integrated with the structural frame. This could possibly lead to significant degradation of stiffness and strength under Strong earthquakes. This paper presents three methods previously proposed and validated by other researchers. Each of these methods has its own system and technique. However, all of them have the same main concept (allowing infill wall–frame interaction under wind loading and minor-to-moderate earthquakes for reduced building drift but disengaging them under damaging events). Each method is adequately explained with summary of its main results. Finally, a comparison of them (including several comparison factors: improved characteristics, preferred infill material, difficulty level of manufacturing and installation, cost, extent of damage under damaging events, etc.) is presented.*

Keywords *Steel frames, Masonry infill, Infilled frames, Cyclic loading, Controlled behaviour.*

I. INTRODUCTION

In steel and concrete moment frame construction, infilling some of the bays with walls made of masonry units is a common practice in many countries. Traditionally, such infill walls are specified by architects as interior or exterior partitions in such a way that they do not contribute to the vertical gravity load-bearing capacity of the structure. However, depending on their construction details, they can adversely influence the seismic behavior of the structure. In other words, under seismic lateral loads the infill walls can interact with the confining frames and take part in resisting lateral in-plane forces and lead to some damage to the wall or frame (e.g., [1,2]). Two methods of construction have been proposed and considered in the literature for infill walls (e.g., [3,4]). The first method is to integrate the infill wall with the structural frame and basically turn it into a shear wall.

The second approach is to isolate the infill wall from the structural frame by leaving gaps between them.

In the case of tight fit construction, depending on the details of their construction (partial vs. complete infill), the infill wall's interaction with the confining frames could possibly lead to premature column failure as a result of the short column effect or to increased levels of unaccounted ductility demand in columns. Furthermore, certain arrangement of the walls can influence the lateral stiffness distribution in plan and elevation, which may result in increased torsional effects and/or soft story situation. As masonry infill walls are usually much stiffer than the structural frame, with increased seismically induced story drift, the tight fit infill walls first experience damage in the form of cracks and separation from the structural frame. Figs. 1 and 2 show some seismic induced failures in buildings as a result of the interaction of tight fit infill walls and frames. Because of such failures, an alternative solution of separating the infill walls from the structural frame by leaving gaps between them is also available as shown in Fig. 3. It is very important to ensure that the gaps, whose required widths are determined analytically, will not be accidentally filled with mortar or other stiff materials during construction procedure. According to Dowrick [4], there are two main performance problems with this approach, which need to be solved. The first issue is to provide convenient details for out-of-plane stability of the infill wall, while the second one is to address the acoustic and fire insulation requirements at the separation gap.

In this paper, three alternative methods previously proposed and validated by other researchers are introduced. The main mutual idea of the three methods is to try to use (to a certain degree) the beneficial effects of strength and stiffness of the infill wall to reduce the story drift during low to moderate seismic events. However, during strong shaking, the proposed systems should seismically isolate the infill wall from the frame in order to prevent failure of the wall (including cracking) as well as damage to the frame.

Finally, a comparison of the three methods (including several comparison factors: the improved characteristics, preferred infill material, difficulty of manufacturing and installation, cost and the extent of damage) was presented. were compared.

Fig. 1 Major damage to the unreinforced masonry infill walls and moderate damage to the columns of an R/C municipal building (Quindia, Colombia 1999 Earthquake, EERI) [11]

Fig. 2 Short column effect due to partial tight fit infill walls in an R/C building (Arequipa, Peru, June 2001 Earthquake, EERI) [11]

Fig. 3 Isolated infill walls from R/C frame with gaps in a recent construction [11]

II. THE FIRST METHOD (SEISMIC INFILL WALL ISOLATOR SUBFRAMES) [11]

M Aliaari et al. [11] proposed a system. In this system, Isolator subframe is attached to the structural frame. The infill wall then is to be constructed within the subframe. The concept of Seismic Infill Wall Isolator Subframe (SIWIS) system is illustrated in Fig. 4, which shows a subframe system including two vertical members and one horizontal member placed between an infill wall and the structural frame. Fig. 5 shows a section through a steel column, where it can be seen that a vertical member of the subframe consists of two sandwiched light- gage steel studs with a "rigid-brittle" element between them. Within the subframe member at the top of the wall, which will not have rigid-brittle elements, and in open spaces of the subframe vertical elements, there can be a flexible filler material that will provide the needed sound insulation and fire-resistance. The out-of-plane stability of the infill wall will be provided through the top subframe member. The location of SIWIS elements shown near the top of the masonry wall panel in Fig. 4 is chosen because the frame will first contact the infill wall at that point under lateral drift and will tend to close the gap if there were no SIWIS elements.

The SIWIS system is designed such that under small to moderate levels of structure frame lateral interface force, the SIWIS "element" will act as a rigid link and transfers the force to the infill wall for the benefit of its stiffness in reducing drift. At larger levels of lateral force (the designed threshold of the subframe), the brittle elements of the subframe break, just like a "fuse", and as a result, the structural frame will be free to displace without transferring force to the infill wall. Different grades (e.g., low, medium, high) for the SIWIS element can be designed and specified according to the strength and stiffness quality of the infill wall. This way, if the infill wall is known to have poor quality or if much of the stiffness of the infill wall is simply not to be relied upon, the mild (low) grade of the SIWIS element will then be suitable. The SIWIS system can be used with many types of masonry infill walls including walls with or without openings, partial or full infills, and with masonry units ranging from high strength concrete masonry blocks and clay brick units to lower strength masonry such as thin wall hollow clay tile units and autoclaved aerated concrete blocks.

A. Preliminary SIWIS element test

The centerpiece of the SIWIS system is an element that rigidly engages the frame to the infill wall interaction under compressive forces between the two. Under large lateral forces to be transferred from the frame to the infill wall, the SIWIS system allows a brittle failure to occur within the element to disengage the contact between the frame and the infill wall. To illustrate this concept, an element was made of three pieces consisting of a steel rod, a concrete disk with a notch, and an open cylindrical PVC piece as the support for the concrete disk [5]. Fig. 6 shows diagrammatic views of the concept of this element and the failure mode of concrete disk along with pictures of its three components that made up the rigid-brittle element for the preliminary testing. Under a certain force level the concrete disk will break along the slanted dashed lines as the rod punches through the disk. An 35.6 kN capacity hydraulic system was used for the tests. Fig. 7(a) sh-

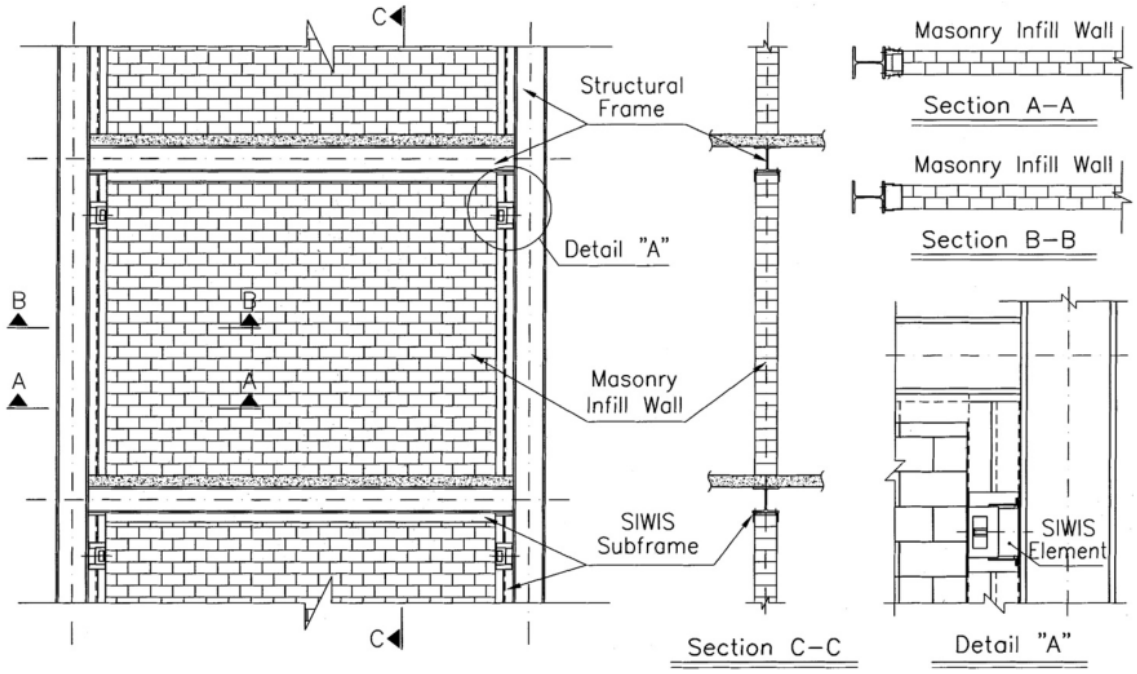

Fig. 4 An example of SIWIS sub frame system used in a building frame [11]

ows the compression test set- up and also identifies the elements of the test set-up.

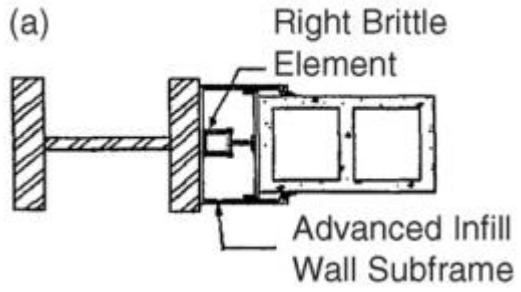

Fig. 5 Details of SIWIS subframe system between infill wall and column from [11]

For preliminary SIWIS element tests, four concrete disks with different disk and notch thickness were tested in order to study the effect of varying the thickness on punching strength. The results of the tests are summarized in Table 1, where it can be seen that it takes a force of 12.5 kN to break the concrete disk used as Specimen C. Fig. 7(b) shows how the steel rod has punched through Specimen C. This level of strength can be thought of to be associated with a low strength SIWIS element. For increased failure capacity, higher strength concrete or thicker disks can be used.

B. Finite element modeling of single-bay, single-story system

In order to investigate the behavior of an infilled frame system including SIWIS elements, its load–deflection response should be compared with the response of the bare frame and the frame with a tightly fitted infill wall. For a more meaningful comparison and verification purposes, initially, a single-bay, single-story steel frame with tightly fitted infill wall that has been the subject of past experimental and analytical studies is considered here. One of the infill wall systems (Specimen WD7) tested by Richardson [6] and reviewed by Dawe and Seah [7] seemed to be a good choice for this analytical study. The specimen had a concrete block

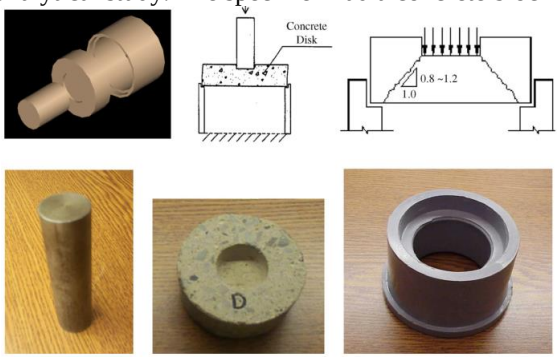

Fig. 6 "Rigid-brittle" SIWIS element and its components including steel rod, concrete disk, and PVC support [11]

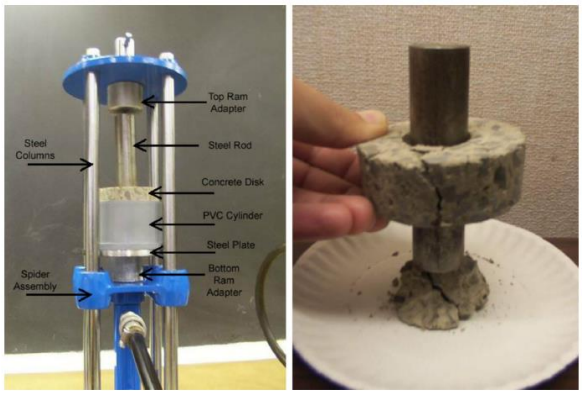

Fig. 7 Pictures of (a) compression test set-up and (b) failure mode of concrete disk after steel rod punches through support [11]

TABLE 1
PRELIMINARY TEST RESULTS OF SIWIS ELEMENT [11]

Specimen	Total thickness (mm)	Notch thickness (mm)	Effective thickness (mm)	Capacity (KN)
A	22.2	7.9	14.3	7.6
B	25.4	6.4	19.0	10.2
C	28.6	7.9	20.7	12.5
D	28.6	9.5	19.1	12.9

masonry infill wall with standard horizontal joint reinforcement and was constructed within the steel frame with no gaps and no ties between the wall ends and the webs of the columns. The finite element modeling approaches used by other researchers have also been found to be useful for comparison purposes in the study reported here.

The study plan consisted of initially modeling the bare frame, then adding brace elements as per the Seah [8] method (single diagonal brace element) and the El-Dakhakhni et al. [9] method (three diagonal brace elements), and finally, developing a model for infilled steel frame with SIWIS system.

For analysis of different nonlinear and two-dimensional models, ANSYS program [10] was used. The steel and masonry wall material properties used for these models were assumed to have modulus of elasticity of 200000 MPa and 16100 MPa, respectively. Moreover, the Poisson's ratio was taken to be 0.3 and 0.15, respectively for steel and masonry. The steel frame members used for the single-bay, single-story modeling are the same as those in [7].

C. Analysis results and discussion for single-bay, single-story system

The four developed finite element models including bare steel frame, single diagonal strut infilled steel frame, three-diagonal strut infilled steel frame, and infilled steel frame with SIWIS system were subjected to incrementally increasing lateral displacement at the top. The resulting lateral load–deflection relations are shown in Fig. 8 along with the existing experimental results for bare frame and infilled frame from [6]. The bare frame response, which is described in the lower part of Fig. 12, fairly accurately matches the available test results.

The capacity of SIWIS element is determined based on the strength of the infill wall. Since the main purpose of the SIWIS system is to save the masonry infill wall from cracking, thus the capacity of SIWIS element needs to be limited to the cracking capacity of the wall panel with an adequate safety margin. For Specimen WD7, the major cracking load was found to be 356 kN [6]. Considering a safety factor of 4, a limiting capacity of 89 kN resulted for the SIWIS element here. In order to observe the effects of varying SIWIS element capacity in the response of the system, three different grades for SIWIS element with capacities of 89 kN, 2×89 = 178 kN, and 3×89 = 267 kN are considered and shown in Fig. 8. It can be seen that the strength provided by SIWIS elements can be increased to desirable levels, although such a capacity should be kept reasonably below the wall cracking capacity.

It can clearly be seen from Fig. 8 that the tightly fitted infill walls demonstrate higher ultimate load capacity than that of the frame with SIWIS element. However, it should be pointed out that the main objective of the SIWIS alternative is to prevent the masonry wall and the frame from sustaining any damage. The conventional tightly fitted masonry infill walls are often very vulnerable to major cracks and even total collapse in moderate to strong earthquakes (e.g., Figs. 1 and 2). The tightly fitted infill wall with load–deflection relation shown in Fig. 12 experienced major cracks at load level of 356 kN [6]. On the other hand, the isolated infill wall with SIWIS element will not experience any failure (e.g., cracks) because of the fuse like performance of the SIWIS element. The impact of this advantage can be

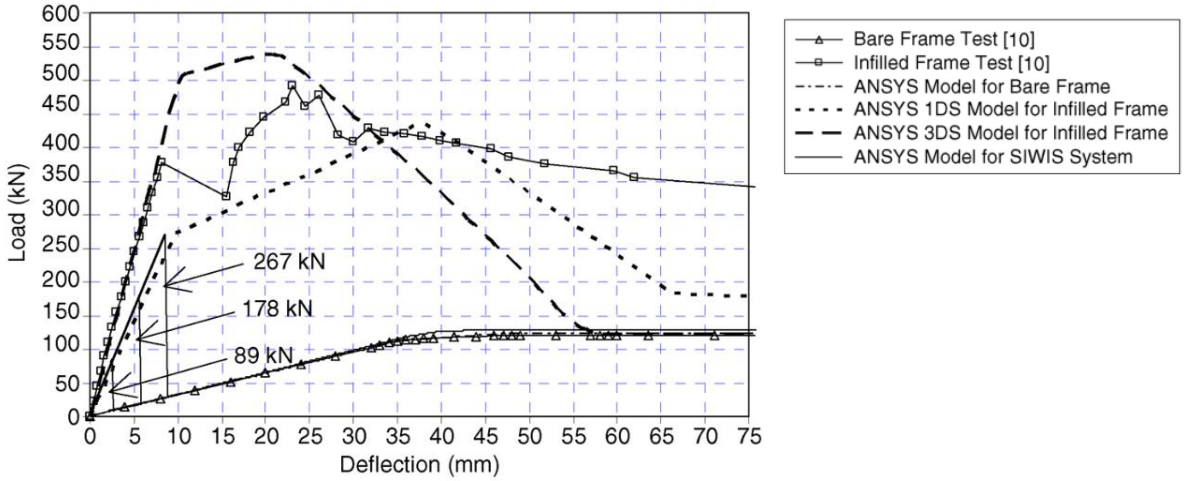

Fig. 8 Load–deflection relation for single-bay, single-story system [11]

higher for infill walls of weaker but lighter material (e.g., hollow clay tile units or autoclaved aerated concrete blocks).

III. THE SECOND METHOD (COMBINING TWO MATERIALS WITH DIFFERENT MECHANICAL PROPERTIES FOR THE INFILL) [18]

Markulak et al. [18] proposed a new structural solution to achieve desirable behavior that combines favourable effects of both structural systems – an increased stiffness, strength and dissipation capacity of the infilled frame system and ductile behavior of the bare steel frame.

This behavior could be provided by combining two materials with different mechanical properties for the infill. The ‘‘weaker’’ material is placed adjacent to the frame and ‘‘stronger’’ fills the rest of the panel, Fig. 12. In that way an infilled frame monolithic behavior could be assured for the service load level (including moderate lateral loading such as wind loads). For higher loadings the steel frame takes over and provides structural stability, without negative infill’s influence. This approach we have tried to utilize in this study. As it was difficult to make an exact prediction of the branching load level, the lightweight AAC blocks were chosen as ‘‘weaker’’ and perforated clay blocks as ‘‘stronger’’ infill material. The AAC blocks were additionally weakened by drilled vertical holes with three different diameters, Fig. 9:

– Specimen CA-1; the hole diameter d = 54 mm.
– Specimen CA-2; the hole diameter d = 74 mm.
– Specimen CA-3; the hole diameter d = 84 mm.

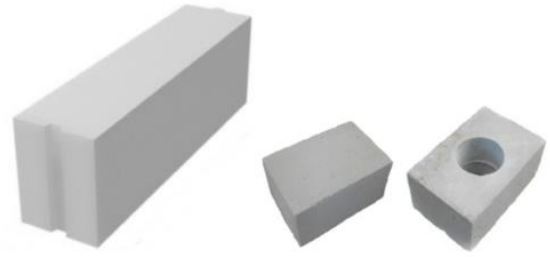

Fig. 9 AAC blocks (‘‘YTONG’’), scaled and drilled block specimens [18]

A. *Testing of steel frames with masonry infill*

Nine one-bay, one-story planar steel frames infilled with masonry and one bare steel frame were built and tested at the Faculty of Civil Engineering, University of Osijek. They were tested under series of quasi-static stepwise increasing loading cycles up to the moment of infill’s and/or frame failure, in accordance with [12].

Tests were performed under the same conditions enabling the comparison of results. All steel frames were identical with rigid frame joints and dimensions as shown in Fig. 21. The specimens were divided into three groups according to the infill type:

(a) Specimens C-i (i = 1–3) were three steel frames infilled with perforated clay blocks (‘‘strong infill’’ with fb= 11.8 MPa, fm= 5.0 MPa, and fk= 1.6 MPa).

(b) Specimens A-i (i = 1–3) were three steel frames infilled with Autoclaved Aerated Concrete blocks (AAC) (‘‘weak infill’’ with fb= 2.0 MPa, fm= 9.1 MPa and fk= 0.9 MPa).

(c) Specimens CA-i (I = 1–3) were three steel frames infilled with a combination of perforated clay blocks and AAC blocks.

(d) Specimen BF was bare steel frame.

Where according to [13], fb is the mean normalized vertical compressive strength of masonry unit, fm is the average compressive strength of mortar and fk is the mean vertical characteristic compressive strength of masonry.

The C-i specimens were tested first, and then A-i specimens and subsequently testing of three steel frames infilled with described combination of perforated clay blocks and AAC blocks (test specimens CA-i) was carried out. All steel frames were identical with rigid frame joints and dimensions as shown in Fig. 10. The frame beams and columns were constructed of HEA 120 standard sections with an area of 25.3 cm2 and moment of inertia of 606.2 cm4. Masonry infill panels used for specimens C-i and CA-i were made of perforated clay. The AAC blocks were used for test models A-i. There was no special connection, outside adhesion, between the frame and masonry infill wall.

The test setup consisted of a heavy steel reaction frame connected to the strong floor and horizontally supported by braces. It was stiff enough to prevent any interaction with the forced response of the specimen being tested. Two hydraulic actuators, of 350 kN capacity and stroke ±150 mm, were fixed to the frame at beam’s level in order to simulate cyclic in plane lateral load. It was applied quasi-statically and cyclically first as force (at the initial stage up to yielding) and then as displacement controlled (after yielding), according to [12].

B. *Experimental results and comments*

The experimental results on C-i specimens showed significantly larger stiffness and strength of the infilled steel frames compared to the bare steel frames and almost smooth shape of the hysteretic curves.

Hysteresis envelope (primary) curves of all tested specimens are given in Fig. 11.

A-i specimens had smaller stiffness (for 60%) than C-i specimens. All C-i specimens had combined diagonal cracking and bed joint sliding shear failure of the infill. The combined mode of failure was observed in A-i test models – bed joint sliding in conjunction with diagonal cracking that was of less intensity in comparison with cracking of perforated clay blocks in test series C-i.

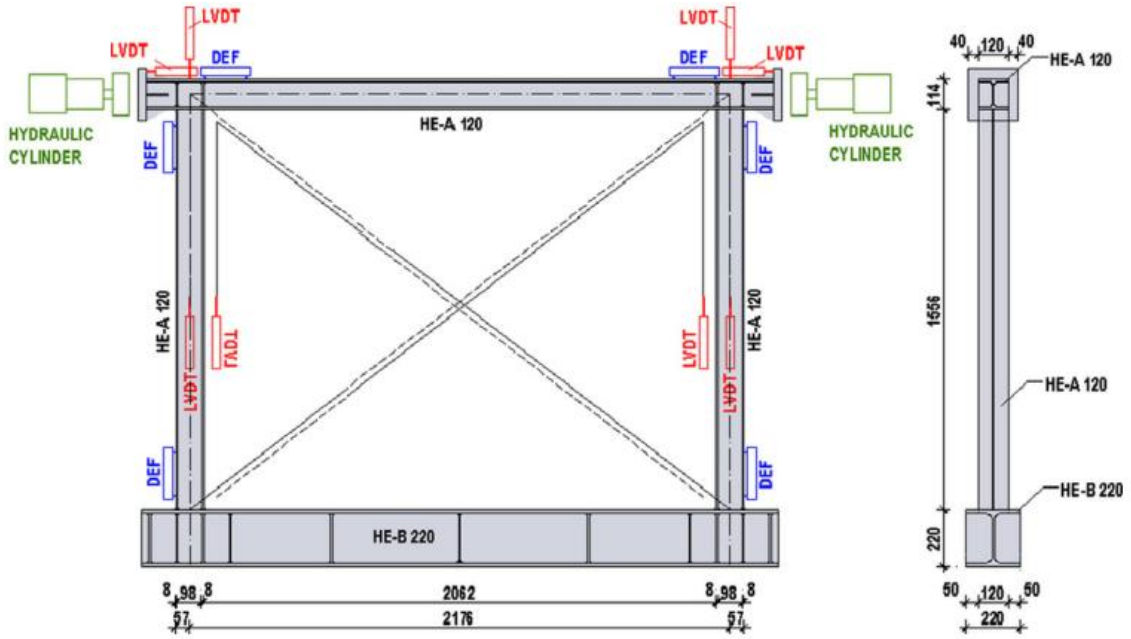

Fig. 10 Dimension of the steel frames and measuring instrumentation [18]

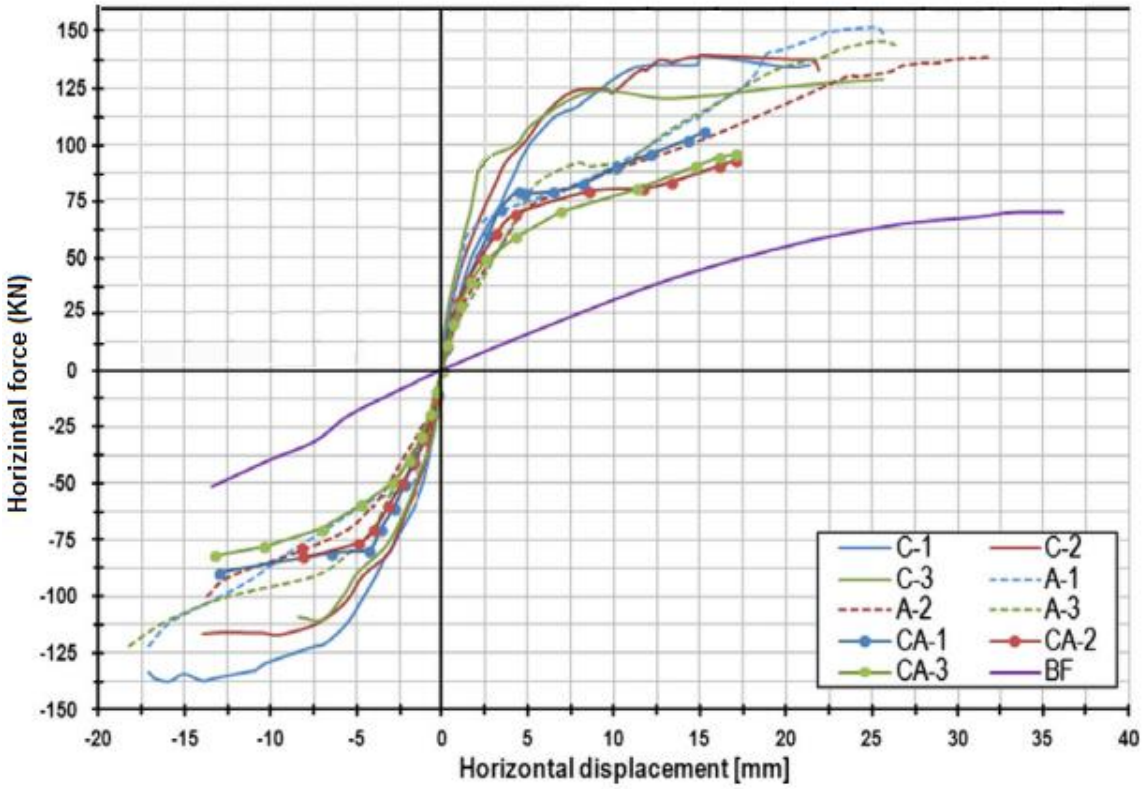

Fig. 11 Hysteresis envelope (primary) curves of all specimens [18]

The hysteresis loops of CA-i specimens had specific shape that indicated two modes of behaviour. This was especially pronounced in the specimen CA-1 and to somewhat lower extent in specimen CA-2. The behaviour of specimen CA-3 was qualitatively similar to that of specimens A-i but the ultimate load was lower. Different properties of drilled AAC blocks placed adjacent to the steel frame in CA-i specimens (the holes had three different diameters d = 54, 74 and 84 mm in specimens CA-1, CA-2 and CA-3 respectively) influenced the behaviour and ultimate loads of particular specimens. The specimen CA-1 and its final crack pattern is shown in Fig. 12.

During the first phase infilled frame acted as one system and had higher stiffness and higher load capacity than bare frame. That phase extended up to the predefined load level (service performance level). In the second phase, when the separation between the infill and frame occurred due to progressive crac-

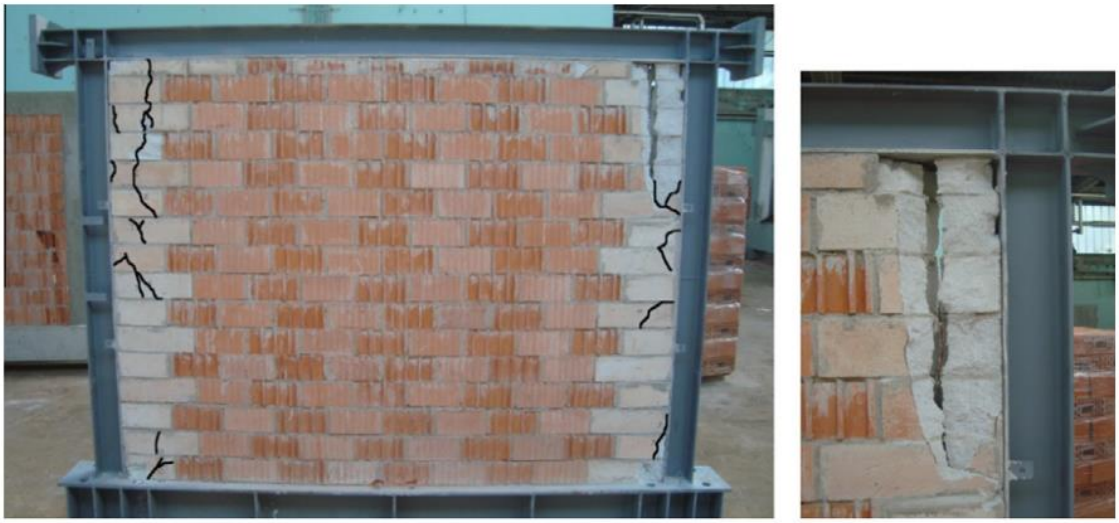

Fig. 11 Photographs of specimen CA-1 [18]

king of weakened masonry area adjacent to the frame, steel flexural action was enabled. That effect is visible in Fig. 13 where the secant stiffness (The stiffness connecting the origin and the point of first sign of damage) degradation corresponding to the subsequent load cycles is given. It can be seen that

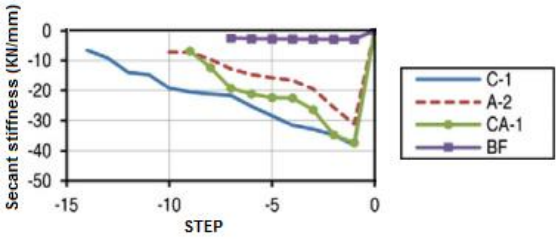

Fig. 13 Secant stiffness degradation [18]

the initial secant stiffness of specimen CA-1 was comparable to the secant stiffness of the specimens C-i. Further increase of the load caused separation between the frame and infill. Stiffness gradually decreased to the stiffness level of specimens A-i.

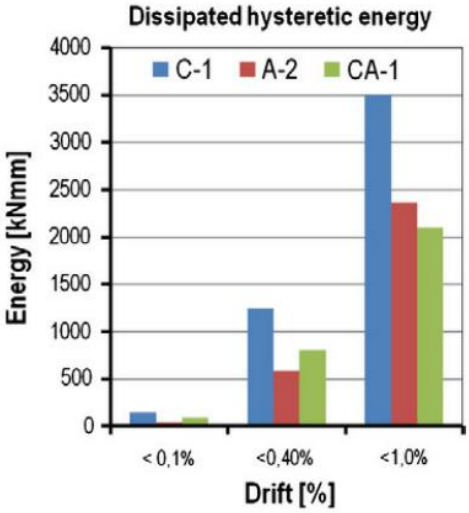

Fig. 14 Dissipated hysteretic energy up to certain drifts [18]

Degradation of the secant stiffness and amount of the dissipated hysteretic energy up to certain drift levels are presented in Fig. 13. and 14. Specimens C-i dissipated about 50% more energy than A-i and CA-i specimens. All three specimen types dissipated much more energy than the bare frame at all drift levels. Total dissipated histeretic energy during test was:

– Specimen C-1 – 5859 kN mm or 6.7 times more than BF.

– Specimen A-2 – 4242 kN mm or 4.8 times more than BF.

– Specimen CA-1 – 2095 kN mm or 2.4 times more than BF.

– Specimen BF – 882 kN mm.

IV. THE THIRD METHOD (INFILLED FRAMES WITH FRICTIONAL SLIDING FUSES) [17]

The two previous methods proposed systems to avoid the interaction (between frame and infill panels) effects, but this method suggested a new system that aims to delay them.

The main characteristic that distinguishes this method from the previous ones is that its system doesn't separate the infill panels from the frame completely, but depends on a new idea. An element is added to the infill, called Frictional Sliding Fuses (FSFs). The fuse acts before infill corner crushing and controls the infill so that it is not overloaded.

Mohammadi et al. [17] experimentally studied the behavior of infills, with a modified sliding layer at their mid-heights. The infill is laid out to accomplish the results of a previous study [14] and to improve the infilled frames' strength, energy dissipation and ductility. In other words, the proposed method eliminates undesirable failure modes and directs damages to have a ductile failure mode. The method is based on the concept of fuses in electrical systems, in which the current is restricted by the fuse. Here, a horizontal layer in infill, named a frictional sliding f-

TABLE 2
EXPERIMENTAL RESULTS PROPERTIES OF THE REAL AND SCALED FRAME [17]

Specimen	Height (m)	Bay width (m)	Column section	Beam section
Real frame	3	4.5	2IPE-400	IPE-400
Scaled frame	1	1.5	IPE-140	IPE-120

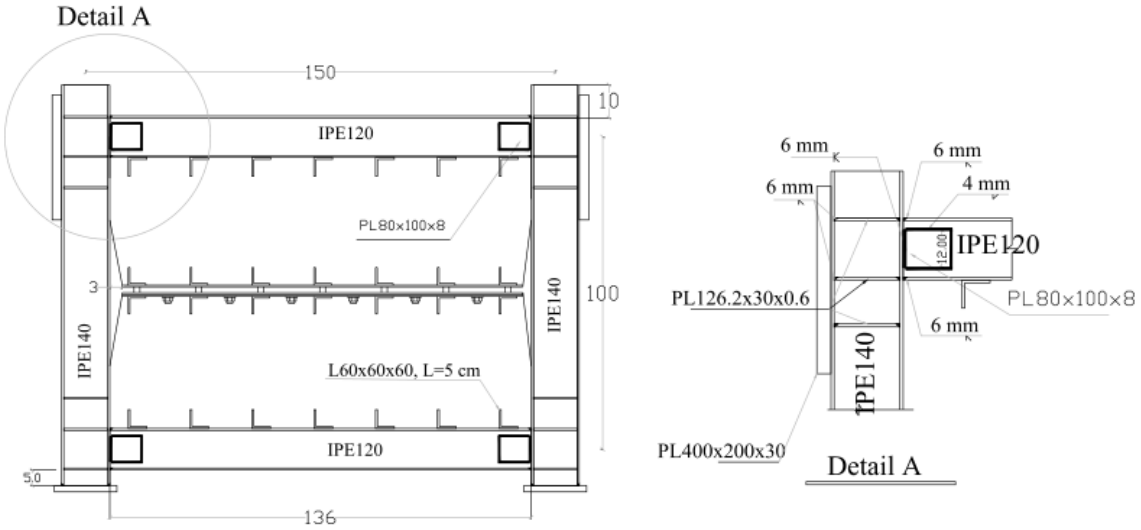

Fig. 15 Details of specimen's frame [17]

use (FSF), slides before infill crushing. The FSF capacity can be adjusted in such a way as not to permit infill crushing. The frictional element restricts the applied load to the infill wall and prevents it from collapsing.

A. Description of specimens

Mohammadi presented the results of cyclic loading tests on three engineered infilled steel frames. Only two specimens are presented herein as the third one results showed the ineffectiveness. The specimens are called EIF-0.35 and EIF-0.5; in all of them an FSF is used to improve their behaviors and adjust their strength capacities. The FSF is a layer with adjustable sliding strength and it will be explained later in this paper. To adjust the FSF, some pre-tensioned bolts are used. The numbers after EIF in EIF-0.35 and EIF-0.5 Signify the ratio of the FSF sliding strength to the ultimate strengths of a similar ordinary infill panel without the FSF, calculated by Mainstone formula [15].

Each specimen consists of a fibrous concrete infill wall, a surrounding steel frame and an FSF at the mid-height. To get the sections of each specimen, a true scaled three-bay four-story Building is designed for a high seismicity zone, based on the Iranian national earthquake code [16]. Then an interior frame of the first story is selected and scaled by the factor of 1/3. The prototype had a steel moment frame, with story heights of 3 m and bay widths of 4.5 m and 5 m in two transversal horizontal directions. The columns and beams of the selected frame in prototype consist of 2IPE-400 and IPE-400 sections, respectively. Based on the scaling rules, the properties of the scaled models were calculated; they are shown in Table 2 in comparison with those of the real structure. The beam–column connections are rigid. Based on analysis, the stiffness of the bare frame is 94.5 kN/cm.

As shown in Fig. 15, the height and length of the frame are 150 cm and 100 cm, respectively. At each corner, three 126.2×30×0.6 mm stiffeners are welded to each side of the column's web to prevent its buckling in high lateral loads. Seven shear connectors (equal leg angle sections, L60×60×6 mm with a length of 50 mm) of 18 cm spacing are used on interior face of each beam and each side of the FSF element to transfer shear forces.

An FSF element is applied at the mid-height of the specimens as shown in Fig. 15. If FSF is used in an infill of normal configuration, the infill will contact the frame at its corner, close to the FSF, after initiation of fuse sliding. Therefore, the infill is chamfered in its corners, near the fuse, with the maximum distance of 3 cm between the fuse and the column (see Fig. 15).

The infill of each specimen is divided into two parts by the FSF, each composed of fibrous concrete and a reinforcing mesh of Φ8 mm bars, with 15 cm horizontal spacing and 10 cm vertical spacing. The modulus of elasticity, yielding and ultimate strengths of Φ8 bars were measured as 1.75 × 105, 320 and 591.8 MPa, respectively.

B. FSF, details and calibration

The FSF is a frictional sliding fuse, composed of three (1360 × 1000 × 60 mm) steel plates, shown in Fig. 16: Two plates (A and B) are fixed to each other, on which the third one (plate C) can slide. Six high-strength N20 bolts connect plates B and C; plate B has slots, as shown in Fig. 16. The slots make sliding

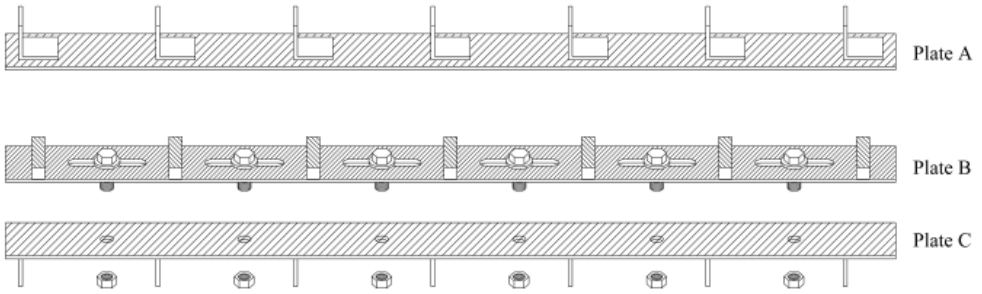

Fig. 26 Detail of FSF elements [17]

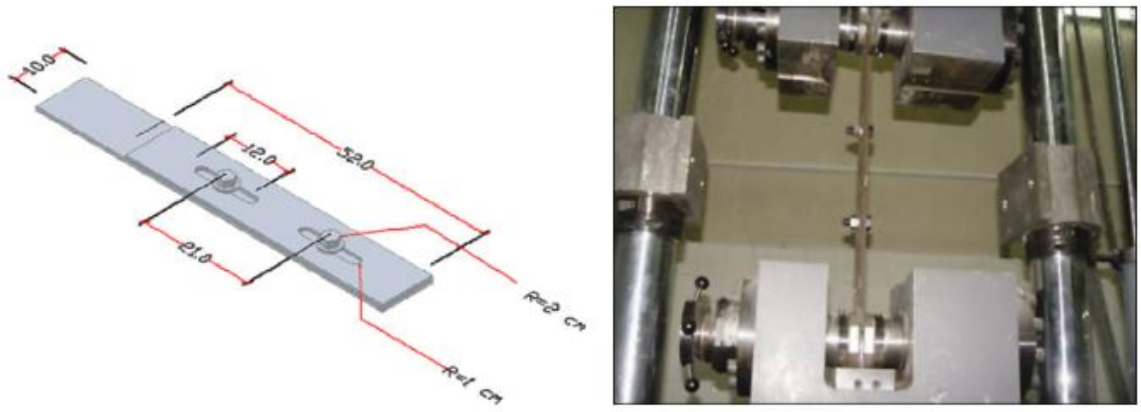

(a) Configuration (dimensions in cm). (b) Testing.

Fig. 37 Calibration fuse under tensile test [17]

possible in the longitudinal direction but restrain transversal movement to prevent out of plane movement of the infill walls. It's worth noting that s-even rectangular sections (20×20×100 mm) are welded to both plates A and B, in order to supply sufficient space for the bolt head during sliding.

The sliding strength of the FSF can be adjusted by regulating the compressive force between the plates, considering the frictional nature of FSF. This can be done through FSF pre-tensioned bolts, which will be explained later.

To adjust the FSF with pre-tensioned bolts, the relation between the tension force and the fastening torque of each bolt should be known.

Five calibration fuses, each with two pre-tensioned bolts, were tested, as shown in Fig. 17. Both bolts of each specimen are fastened with the same torque and the sliding strength is obtained from a tensile loading test, shown in part (b) of Fig. 18.

A force–displacement diagram of the specimens is shown in Fig. 18(a), in which the fastening torques corresponding to the bolts of each calibration fuse are shown by the expression ''T='' . Fig. 18(b) shows the results briefly, in which the fuses' sliding strengths are plotted via the bolts' fastening torques, compared with the analytical ones.

Regulating the FSF bolts leads to adjust the specimens. This may be employed where higher strengths, than those obtained by adjusting the fuse bolts, are required, e.g. in rehabilitation projects.

In specimens EIF-0.35 and EIF-0.5, the bolts are

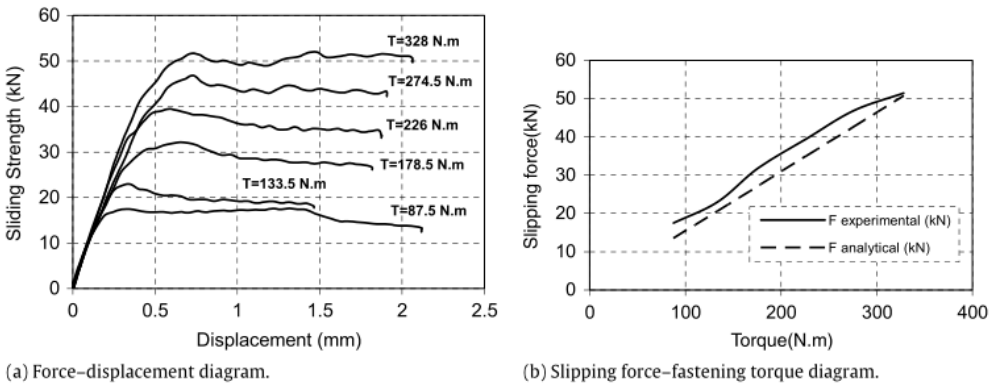

(a) Force–displacement diagram. (b) Slipping force–fastening torque diagram.

Fig. 48 Results of tensile tests on calibration fuses [17]

regulated to adjust the FSF for sliding strengths of 51 kN and 73 kN, respectively. Based on the results of the calibration fuses, shown in Fig. 18, the required fastening torques for the FSF bolts of EIF-0.35 and EIF-0.5 are calculated as 87.5 and 140 N m, respectively.

Displacement controlled loading is applied to the specimens by a hydraulic jack, controlled by a computer. The specimens are subjected to some loading cycles. Lateral supports are provided at two points of the upper beam to prevent out of plane behavior.

C. Test results

In this section, the results of the experimental tests on specimens are presented. During the tests on EIF-0.35 and EIF-0.5, frame–infill interface cracking occurred initially. Then inclined cracking started near the shear connectors and spread throughout the top and bottom parts of the wall at an angle of 45° as shown in Fig. 19.

In EIF-0.35, the FSF sliding started at the 17th cycle under a lateral load and drift of 80.28 kN and 0.389%, respectively. For EIF-0.5 the sliding was at the 30th cycle with a load and drift of 136.9 kN and 0.53%.

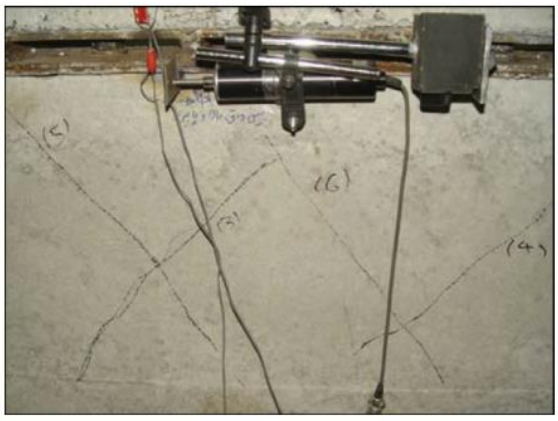

Fig. 19 Inclined cracks at the infill in EIF-0.35 [17]

The FSF sliding strengths and test results of all specimens are listed in Table 3, including initial

(a) Corner crushing and shear failure of infill. (b) Plastic hinge in the top beam.

Fig. 50 Failure modes of specimens EIF-0.35 and EIF-0.5 [17]

TABLE 3
PROPERTIES AND RESULTS OF THE EXPERIMENTAL TESTS [17]

Specimen	SFS sliding strength (kN)	Initial Stiffness (kN/mm)	SFS sliding Strength (kN)	Infill cracking Strength (kN)	Ultimate Strength (kN)
EIF-0.35	51	24.3	80.28	50	267.6
EIF-0.5	73	31.86	136.9	60	314.7

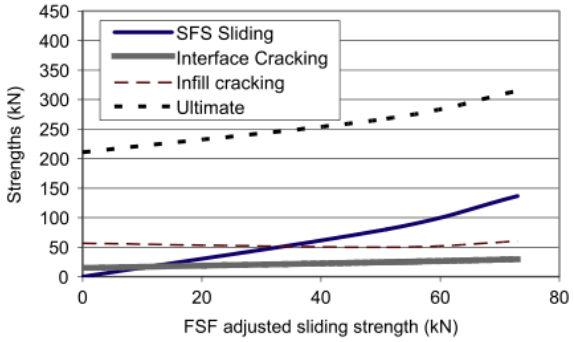

Fig. 21 Comparison of strengths with FSF adjusted sliding strength [17]

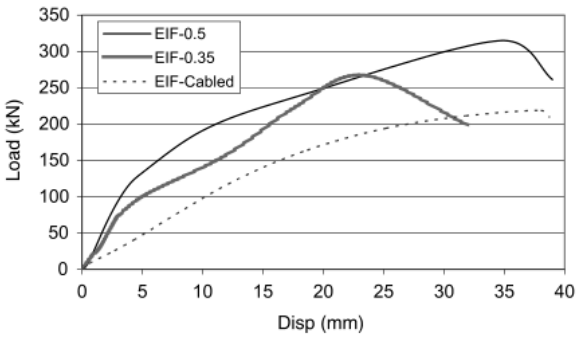

Fig. 22 Comparison of strengths with FSF adjusted sliding strength [17]

stiffness, as well as the strengths and drifts (displacement/story height) of the interface cracking, infill cracking and ultimate case.

The variation of strengths corresponding to interface cracking, FSF sliding, infill cracking and ultimate case are compared with the FSF adjusted sliding strength in Fig. 21.

As shown, both the strengths of FSF sliding and ultimate cases increase on increasing the FSF strength. However, the strengths of interface cracking or infill cracking do not correlate with the SFS strength.

The envelops of Hysteresis diagrams of the specimens are shown in Fig. 22.

Based on the experimental results, it can be concluded that the ultimate strength of the specimens have been increased by using the FSF, compared with an ordinary infilled frame of similar dimensions and materials. According to previous investigations [19], the Mainstone formula [15] estimates the ultimate strength of infilled frames accurately. Based on this formula, the ultimate strength of an ordinary infilled frame, without an FSF, is almost 145 kN. However, the ultimate strengths of EIF-0.35 and EIF-0.5 are 267.6 and 314.7 kN, respectively, which are at least 84.5% higher.

Comparison of the results shows that the more the FSF sliding strength is the stronger the infill gets: EIF-0.5 with the greatest FSF sliding strength has the highest ultimate strength.

Moreover, application of an FSF increases the deformation capacity of infilled frames. The deformation capacities of the specimens have improved considerably, in comparison with a similar ordinary infilled frame. According to previous research, the corresponding drift of the ultimate strength for an ordinary infill panel is between 0.12% and 0.79% [20,21]. Another experimental study has shown that the ultimate drift is 0.32% for concrete infills and 0.5% for fibrous concrete ones [19]. However, based on the results of the present study (Table 3), the deformation capacities of the specimens are more that 2.5%. This means that the deformation capacity of a fused infilled frame is at least five times that of an ordinary similar one.

V. Comparison and Conclusions

This paper presents three methods previously proposed and validated by other researchers. Each of these methods has its own system and technique. However, all of them have the same main concept (allowing infill wall–frame interaction under wind loading and minor-to-moderate earthquakes for reduced building drift but disengaging them under damaging events). Each method is adequately explained with a summary of its main results.

A comparison of the three methods (including several comparison factors: improved characteristics, preferred infill material, difficulty level of manufacturing and installation, cost, extent of damage under damaging events, etc.) is presented in Table 4.

Acknowledgment

The research presented in this paper is supported by Faculty of Engineering at Tanta University, in Egypt and its support is gratefully acknowledged.

References

[1] Drysdale RG, Hamid AA, Baker LR. Masonry structures—behavior and design. 2nd ed. The Masonry Society; 1999.
[2] Paulay T, Priestley MJN. Seismic design of reinforced concrete and masonry buildings. Wiley; 1992.
[3] Tomazevic M. Earthquake-resistant design of masonry buildings. London: Imperial College Press; 1999.
[4] Dowrick DJ. Earthquake resistant design for engineers and architects. 2nd ed. Wiley; 1987.
[5] Memari AM, Aliaari M. Seismic infill wall isolator subframe (SIWIS) system for use in buildings. In: Proceeding, ATC-17-2 seismic on response modification technologies for performance-based design. 2002.
[6] Richardson J. The behavior of masonry infilled steel frames. MS thesis. University of New Brunswick, Fredericton, NB Canada; 1986.
[7] Dawe JL, Seah CK. Behavior of masonry infilled steel frames. Canadian Journal of Civil Engineering 1989;16:865–76.
[8] Seah CK. A universal approach for the analysis and design of masonry infilled frame structures. Ph.D. thesis. University of New Brunswick, Fredericton, NB Canada; 1998.
[9] El-Dakhakhni WW, Elgaaly M, Hamid AA. Three-strut model for concrete masonry-infilled steel frames. Journal of Structural Engineering, ASCE 2003;129:177–85.
[10] ANSYS user's manual—version 6.1. Canonsburg (PA): ANSYS Inc.;2002.
[11] M. Aliaari, A.M. Memari. Analysis of masonry infilled steel frames with seismic isolator subframes. Engineering Structures, 2005;27: 487–500.
[12] Federal Emergency Management Agency (FEMA). FEMA 461, interim testing protocols for determining the seismic performance characteristics of structural and nonstructural components. Washington, DC: Federal Emergency Management Agency; 2007.
[13] European Committee for Standardization (CEN). EN 1996-1-1, Eurocode 6: design of masonry structures – Part 1-1: general rules for reinforced and unreinforced masonry structures. Brussels, Belgium: CEN; 2005.
[14] Mohammadi MGh. Methods to improve mechanical properties of infilled frames. Ph.D. thesis. Tehran (Islamic Republic of Iran): Civil department, Sharif University; 2007.
[15] FEMA 306. Evaluation of earthquake damaged concrete and masonry wall buildings. Applied technology council, ATC-43 Project, 1998.
[16] Iranian Code of practice for seismic resistant design of buildings. 3rd ed. Standard No. 2800-05. Building and Housing Research Center, BHRC-PN S 253. 2007.
[17] M. Mohammadi, V. Akrami. An engineered infilled frame: Behavior and calibration. Journal of Constructional Steel Research, 2010;66: 842–849.
[18] D. Markulak, Ivan Radic´, Vladimir Sigmund. Cyclic testing of single bay steel frames with various types of masonry infill. Engineering Structures, 2013;51: 267–277.
[19] Mohammadi MGh. Stiffness and damping of single and multi-layer infilled steel frames. Journal of ICE Structures and Buildings 2007;160:105–18 [Paper No. 14599].
[20] Moghadam HA, Dowling PJ. The state of the art in infilled frames, ESEE Research Report No. 87-2, 1987.

TABLE 4
A COMPARISON OF THE THREE METHODS

	Method 1	Method 2	Method 3
Main idea	Seismic Infill Wall Isolator Subframe (SIWIS) with a "rigid-brittle" element	combining two materials with different mechanical properties for the infill	an element is added to the infill, called Frictional Sliding Fuses (FSFs)
Behavior and characteristics of the proposed system	* the stiffness of the infilled frame with SIWIS elements before failure of SIWIS element is about 10 times that of the bare frame, but 75% of the stiffness of frame with tightly fitted infill wall. * the tightly fitted infill walls demonstrate higher ultimate load capacity than that of the frame with SIWIS element.	* lateral load capacity of the proposed system was almost the same as that of the frame infilled with lightweight AAC blocks until the moment when the separation occurred. Then the frame and infill behaved as two, almost independent elements. * the proposed system dissipated about 240%, 36% of the energy dissipated by the bare frame and the frame infilled with perforated clay blocks, respectively.	* the ultimate strengths of the proposed engineered infilled frame are at least 84.5% higher than the ordinary infilled frame * the deformation capacity of the engineered infilled frame is at least five times that of an ordinary similar one.
Preferred infill material	any type of masonry units ranging from high strength concrete masonry blocks to lower strength masonry	Two types of infills: * weaker material is placed adjacent to the frame (e.g., AAC blocks) * stronger one is at the rest of the panel (e.g., clay blocks)	high strength infill (e.g., fibrous concrete infill)
Difficulty level of installation & manufacturing	difficult to manufacture and install	easy to install	very difficult to manufacture and install
Cost	moderate	low	high
infill's detrimental effects	prevented	Delayed	
Extent of damage under damaging events	no failure or cracks		As the loading amplitudes increase, infill corner crushing occurs, followed by infill horizontal shear failure near the beams

[21] Mehrabi AB, Shing PB, Schuller MP, Noland JL. Experimental evaluation of masonry infilled RC frames. Journal of Structural engineering 1996;122(3).